

SILICA-MOUNTED FTIR-ACTIVE ORGANOMETALCARBONYL DERIVATIVES AS FUNCTIONAL MATERIALS

C. E. Anson^{a†}, T. J. Baldwin^a, N. J. Clayden^a, C. S. Creaser^b, O. Egyed^{b,††}, M. A. Fey^a,
W. E. Hutchinson^b, A. Kavanagh^a, G. R. Stephenson^{a*}, P. I. Walker^a

^aWolfson Materials and Catalysis Centre, School of Chemical Sciences and Pharmacy,
University of East Anglia, Norwich, NR4 7TJ, UK

^bSchool of Science, Nottingham Trent University, Clifton Lane, Nottingham, NG11 8NS, UK

Organometalcarbonyl complexes adsorbed onto silica and covalently attached to ~63 μm , ~15 μm and ~7 nm diameter silica particles have been studied by IR and ²⁹Si MAS NMR. The properties of the characteristic vibrational stretching modes of the M-CO groups examined by FTIR spectroscopy using ATR, DRIFT, and an optrode assembly, are discussed. In the ²⁹Si NMR spectra, an additional signal in the -20 ppm region was observed in the presence of the covalently attached organometallic, and the intensity of the Q³ band shoulder of the main bulk Q⁴ silica signal at -110 ppm was reduced in intensity. Determination of surface loading of the silica by microanalysis, AA, DRIFT and ²⁹Si NMR is compared. The FTIR spectra are compared by the use of Bellamy plots, and normalised differential response ratios are used to quantify the contributions of environmental effects on the relative positions of the $\nu(\text{CO})$ vibrational stretching modes of organometallic complexes. The terms Δ_R and Δ_N are defined.

(Received July 10, 2003; accepted July 31, 2003)

Keywords: Organometalcarbonyl sensors, Environment sensitivity, Supported organometallics, ²⁹Si NMR, FTIR optrode, Bellamy plots

1. Introduction

New generations of advanced functional materials need to out-perform the capabilities of current methods. Molecular sensors can be constructed (Fig. 1c) from molecular receptors (Fig. 1b) by attaching additional functionality in the form of a signal transduction portion of the molecule [1], but the performance of such designs is normally limited by the selectivity of the receptor. Thus where similar analytes compete for binding in the receptor, there is a lack of discriminating power in the sensor, and the optimisation of the host-guest chemistry of the receptor for a specific analyte is often far from straightforward. Furthermore, this approach requires the design and synthesis of an optimised receptor for each analyte, a time-consuming process and one that does not provide a sensor that can be applied to each of a range of similar analytes. Our approach (Fig. 1d) to this problem has been to exploit the intense narrow vibrational bands of carbonylmetal complexes.

Compared to typical and currently popular signal transduction systems such as UV [2] and fluorescence [3] spectroscopy or electrochemistry [4], the advantage of IR spectroscopy is that the

* Corresponding author: g.r.stephenson@uea.ac.uk

† Present address: Institut für Anorganische Chemie II, Universität Karlsruhe, Engesserstrasse Geb. 30.45, 76128 Karlsruhe, Germany

†† Present address: Chemical Research Center of the Hungarian Academy of Sciences, PO Box 17, H-1525, Budapest, Hungary

signals of several organometallic complexes can be determined independently but in a single spectroscopic experiment. The vibrational bands are sufficiently narrow that combinations of complexes can be chosen to give signals that do not overlap, i.e. a “multi-carbonylmetal” method. We have employed [5] this approach for pH determination using an ionisable group in electronic communication with organometalcarbonyl complexes, and the vibrational-spectroscopy-based bioanalysis method CMIA [6] has been modified [7] to demonstrate the capabilities of multi-CMIA, visualising the responses of several independent M-CO signals in a single process.

There is, however, a second and distinct method to extract analytical information from the carbonylmetal portion of our molecular sensors. Not only the position but also the shape of the bands is influenced by changes in the environment of the complex [8], and the occupancy of the molecular receptor [9-11]. We have applied this to measure concentrations of alkali metals [9] and organic analytes such as herbicides and barbiturates [10]. In a study [11] of π stacking effects, binding to a receptor and through-space environment effects have been detected and distinguished. Because of the well defined nature of the IR signals, PCA (Principal Component Analysis) can be used to distinguish separate influences from different analytes [8, 9, 12], and the combination of PCA and multi-carbonylmetal methods will give receptors of exceptional discriminatory power and generality of application.

A recent development in our work has been the attachment of our organometalcarbonyl systems to silica nanoparticles for use with ATR cells [12] and the ATR tip of an optrode [13] employing fibre optics (Fig. 1e) to separate the sensing component from the sample-well of the spectrometer. Supported organometallics can be coated onto the optrode by a simple procedure of dipping into colloidal suspensions of particles, and after use, the coating can be wiped off, and the probe re-coated for the next analysis. Single sensors, or mixtures of sensors for multi-response experiments can be coated onto the ATR tip, and the full effectiveness of peak-shift and PCA methods has been demonstrated for the supported organometallics and for the optrode system, using simple tricarbonyliron 5-aminocyclohexadiene complexes.

We now describe further details of the development of the solid-support procedures that has enabled the construction of the optrode device, the extension of these methods to functionalised systems with $-\text{CO}_2\text{Me}$, $-(\text{C}_6\text{H}_5)_2\text{CH}_2$ and $-\text{CH}_2\text{CH}_2\text{CO}_2\text{Me}$ groups as substituents on the cyclohexadiene ring, and comparisons by means of Bellamy plots [15, 16] of the differential responses of an extended range of organometallic structures, both in solution and in supported form, in work that defines the capabilities needed for further multi-response procedures with organometalcarbonyl-based molecular sensors as advanced functional materials in analytical applications.

2. Experimental

2.1. Materials

3-(Diethoxymethylsilyl)propylamine, potassium hydroxide, cyclohexanol, dodecane and fumed silica were supplied by Aldrich Chemical Company (Gillingham, Dorset, UK), and used as received. Other solvents were obtained from Rathburn Chemicals Limited (Walkerburn, Scotland) and were of analytical reagent grade. Silica as 60 mesh and 40 mesh grades were purchased from Fluka (Gillingham, Dorset, UK / Buchs, Germany). The complexes **5** [17], **16** [18], **17** [19], and **18** [20] (Fig. 2) were prepared by the reported procedures.

2.2. Adsorption of organometallic complexes onto silica

In a typical experiment, tricarbonyl(η^4 -1-methoxycyclohexadiene)iron(0) (**1**) or tricarbonyl(η^4 -1,4-dimethoxycyclohexadiene)iron(0) (**3**) was dissolved in an excess of dichloromethane and this solution was then added to a known mass of silica gel (Fluka 60734, silica gel 40, average particle size 5-15 μm , surface area 600 $\text{m}^2 \text{g}^{-1}$). The solvent was removed using a rotary evaporator and the dry, coated silica gel was stored under a nitrogen atmosphere. Spectra of the dry coated silica gel, at different levels of coating in the region 0.5-5.0 % (w/w), were measured using the Baseline DRIFT cell (SpectraTech Inc.). All spectra measured were the result of averaging 64 scans after referencing against a background spectrum of the pure, uncoated silica gel. A resolution of 2 cm^{-1} was used with the liquid nitrogen cooled InSb detector.

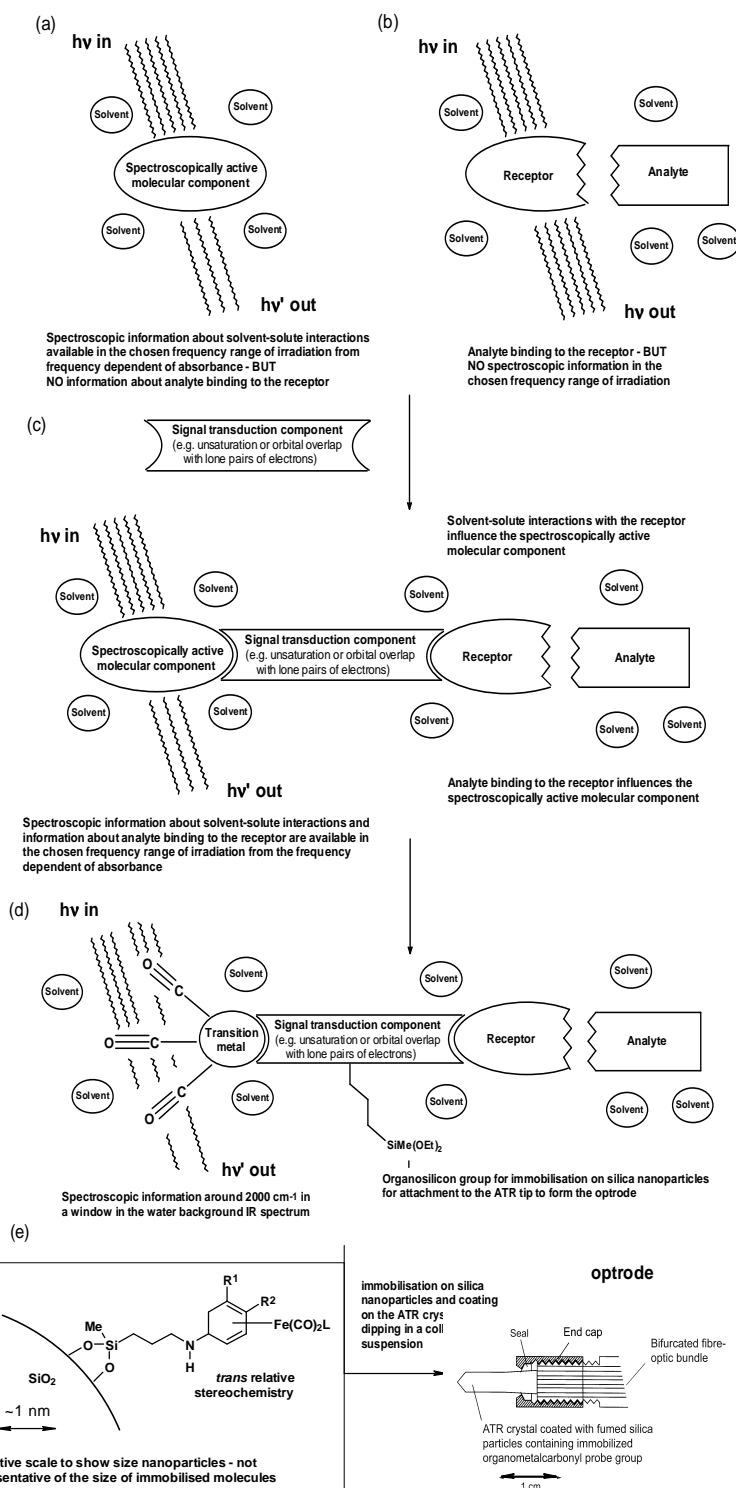


Fig. 1. Cartoon to illustrate the stages of the ten year development of IR-active optrode-mounted molecular sensors [14]: (a) our investigations of spectroscopic properties and preparative chemistry of organometalcarbonyl complexes [8]; (b) the science of host-guest chemistry and (c) concepts of molecular sensor construction: signal transduction [1]; (d) the development in our work of molecular sensors containing carbonylmetal complexes with capabilities for mounting on a solid support; (e) attachment of our organometalcarbonyl-based sensors on silica nanoparticles and coating onto ATR crystals [13] and the optrode tip [14] – simple reusable IR-active sensing devices (inset shows an organometalcarbonyl complex immobilised on silica).

2.3. General procedure for covalent attachment of the tricarbonyliron complexes to silica

Silica gel (60 mesh, $300 \text{ m}^2 \text{ g}^{-1}$), 40 mesh silica ($600 \text{ m}^2 \text{ g}^{-1}$), or fumed silica (average particle size 7 nm, surface area $380 \text{ m}^2 \text{ g}^{-1}$) was dried for 2 hours at $350\text{-}500 \text{ }^\circ\text{C}$ in air. A solution of the silylaminoalkyl-substituted organoiron complex (0.2 g, 0.57 mmol) was prepared by reaction of the corresponding cyclohexadienyliron complex with $\text{H}_2\text{NCH}_2\text{CH}_2\text{CH}_2\text{SiMe}(\text{OEt})_2$ in dry dichloromethane (1-2 ml) and added directly to the silica (1 g, 16 mmol) in a flask under an atmosphere of nitrogen. The slurry was mixed thoroughly by sonication for 10 minutes. The solvent was pumped off, and the residue was washed with toluene, methanol and n-hexane, and then dried under vacuum at $70 \text{ }^\circ\text{C}$ to afford the silica-supported organoiron complex.

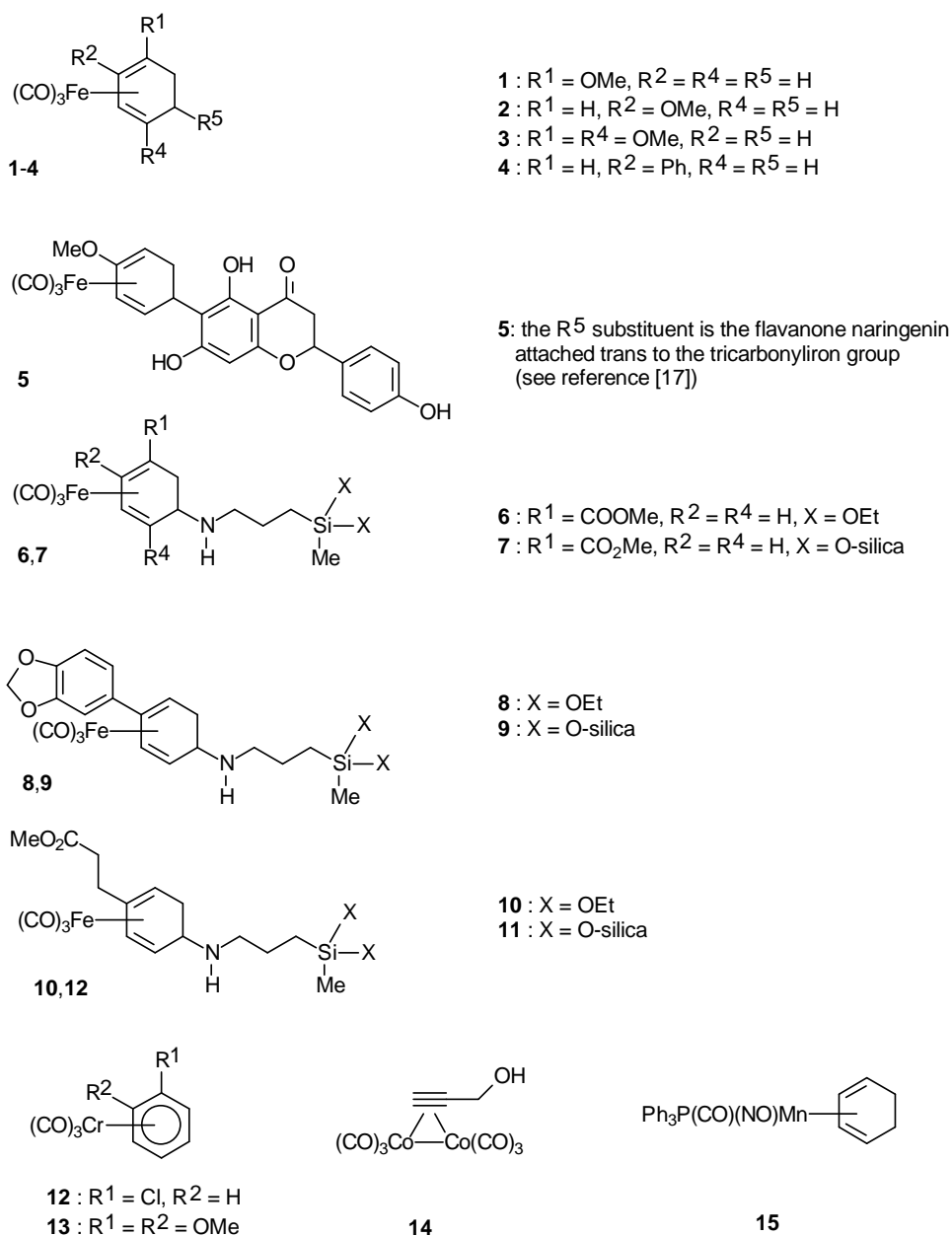


Fig. 2. Organometalcarbonyl complexes for spectroscopic studies including examples derivatised for use in biological investigations (5) and surface mounting experiments (6, 8 and 10).

2.4. Atomic absorption spectroscopy

The organometalcarbonyl loading on the silica was estimated using the following methods:

Method A [13]: The coated fumed silica (0.338 g) was dissolved in 0.1 M potassium hydroxide (100 ml). A blank was prepared by dissolving uncoated silica (0.034 g) into 10 ml of 1 M potassium hydroxide solution. The iron concentration in the extracts was determined by atomic absorption using a Perkin Elmer 3110 spectrometer at 372.0 nm with standard additions (1-3 ppm). The resulting calibration graph was extrapolated to give the concentration of iron in solution, from which the amount of complex on the silica and hence the organometallic complex loading was calculated.

Method B: The coated silica (0.2 g) was dissolved in concentrated nitric acid (10 ml). Calcium chloride (0.5 mg) and milli-Q water (10 ml) were added. The mixture was heated at 75 °C for 3 min, cooled and filtered into a volumetric flask, and made up to 100 ml with milli-Q water. Analysis was performed using a Perkin Elmer 3300 spectrometer at 248.3 nm, with calibration by the method of standard additions using standards (1-200 ppm) in a similar fashion to method A.

2.5. FTIR spectroscopy

IR spectra were recorded using Omnic™ IR software on a Perkin Elmer 1720X spectrometer, a Nicolet 410-Impact spectrometer, or a Nicolet Magna 750 spectrometer and fitted with a liquid nitrogen cooled InSb nitrogen cooled InSb detector. Spectra were recorded at resolutions between 0.5 and 4 cm⁻¹.

Solution IR: In a typical procedure, tricarbonyl(η^4 -1,4-dimethoxycyclohexadiene)iron(0) (**3**) was dissolved into different solvents at the same concentration (3.3×10^{-3} M). The FTIR spectra were measured using a liquid cell (SpectraTech Inc.) with a pathlength of 0.5 mm at a resolution of 0.5 cm⁻¹ with an InSb detector. A total of 16 scans were averaged for each final spectrum. The liquid cell transmission windows were constructed from ZnSe. Solution spectra measured in a divided cell, used an apparatus constructed by placing a spacers of 0.1 and 0.2 mm each side of a PTFE semipermeable membrane. The 0.1 mm spacer created a void to hold the silica gel coated with 1% (w/w) tricarbonyl(η^4 -1-methoxycyclohexadiene)iron(0), and a spacer of 0.2 mm was used for the liquid flow-through space. A resolution of 2 cm⁻¹ was used and sample spectra were ratioed against uncoated silica gel in the same solvent system.

IR spectra in KBr disks were prepared by mixing the silica sample and powdered KBr in a 1:10 ratio and pressing at approximately 8-10 metric tons for 5-6 mins, using a standard laboratory KBr press. Transmission spectra were recorded against a background of air at 1 cm⁻¹ resolution using 64 scans.

DRIFT measured at 2 cm⁻¹ using the Baseline DRIFT cell (SpectraTech Inc.) or a Phillips Scientific DRIFT array unit (at 1 cm⁻¹).

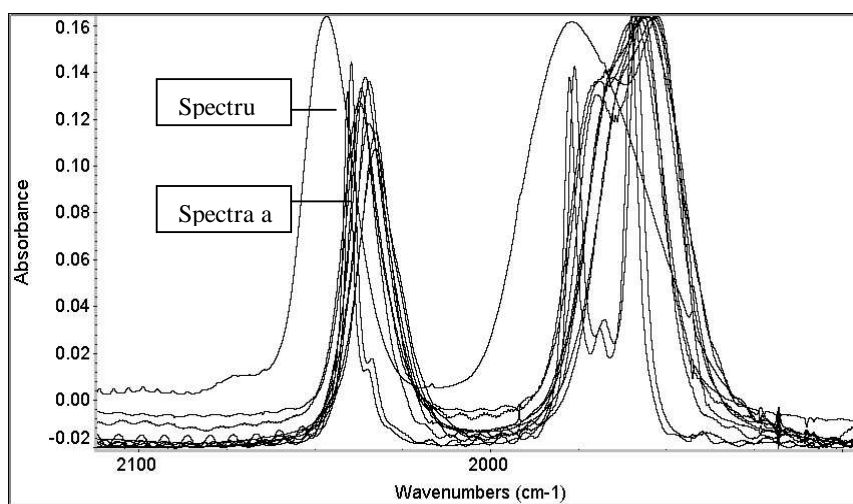
Horizontal ATR FTIR spectra were measured using a Baseline horizontal attenuated total reflection accessory (SpectraTech) containing a ZnSe crystal that presented an incidence angle of 45°. Each spectrum was a result of averaging 32 scans.

Optrode: The construction of the optrode device (Fig. 1e) has been reported previously [14]. The device uses an enhanced fibre optic attenuated total reflectance (ATR) accessory (Remspec Corporation, MA), which consists of a ZnSe internal reflectance element located at the end of a bifurcated IR-transparent optical fibre bundle encased within a stainless steel probe. The fibres are interfaced to the FTIR spectrometer through a launch system located in the spectrometer sample compartment and incorporating two gold plated mirrors which focus the light from the IR source onto the end of optical fibre bundle and then collect and focus reflected radiation onto the detector. Spectra were recorded at 4 cm⁻¹ resolution. The ATR element was coated with fumed silica containing the immobilized organometalcarbonyl probe groups by repeated dipping into a colloidal solution prepared by sonication.

2.6. Solid state MAS ^{29}Si NMR spectroscopy

Solid state ^{29}Si NMR spectra were acquired on a Bruker MSL-200 NMR spectrometer operating at 39.73 MHz. Magic angle sample spinning (MAS) was carried out using a Bruker double bearing rotor system with 7 mm zirconia rotors. Typical spinning speeds were 4 kHz, which was sufficient to make the spinning sidebands of low intensity and outside the region of interest. A 72° pulse at 4 μs together with recycle delay of 60 s was used over a spectral width of 20 kHz, collecting between 1300 and 5000 transients for each sample to obtain an acceptable signal to noise ratio. The choice of recycle delay was based on a trial experiments examining the Q^3+Q^4 band region of a sample of underivatized 60 mesh silica, choosing the shortest value that still avoided complications from spin saturation. The siloxane Q_8M_8 was employed as a ^{29}Si external secondary reference, taking the M type resonance as +11.5 relative to tetramethylsilane.

(a)



(b)

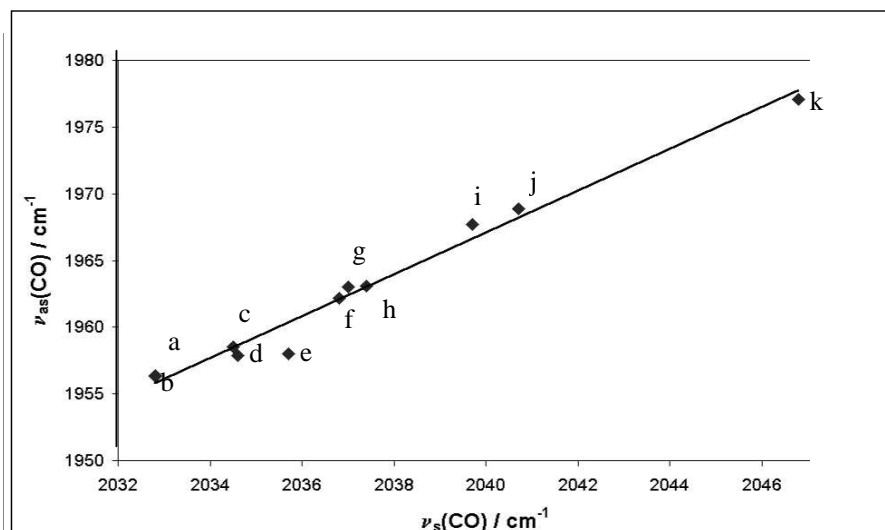


Fig. 3. a) Overlaid FTIR spectra of tricarbonyl(η^4 -1,4-dimethoxycyclohexadiene)iron(0) (**3**) in ten different solvents: a, acetone; b, tetrahydrofuran; c, toluene; d, ethyl acetate; e, dichloromethane; f, diethylether; g, butanol; h, propanol; i, dodecane; j, hexane; and, k, on silica gel. b) Bellamy-type plot to show environment-dependence of the IR spectra of complex **3** using the data from Fig. 3a.

3. Results and discussion

3.1. FTIR studies of organometalcarbonyl complexes in solution

Our initial study [8] of the environment sensitivity of IR-active carbonylmetal complexes used Bellamy plots of $\nu_s(\text{CO})$ against $\nu_{as}(\text{CO})$ vibrational modes [16] to demonstrate that solvents of different polarities produce spectra in which the positions of the centres of the vibrational bands are shifted substantially relative to one another, but correlate to a linear plot in which the responses to each solvent are spread out along the diagonal between hexane and DMA. The data from our original study [8] of **1** in thirteen different solvents has been extended in this work by a similarly detailed study of **2** and **3** (Fig. 3), and in a shorter survey of a range of types of metal complexes to enable comparisons to be made. In order to place the properties of these all these complexes on the same graph, band positions were calculated in terms of relative wavenumbers for symmetric and antisymmetric vibrational modes. For each complex, these relative positions were obtained by subtracting the observed position of each vibrational band from that measured for hexane. Hexane was chosen as the primary reference solvent for this purpose because the typically narrow nature of $\nu(\text{CO})$ vibrational bands allows the position of the band to be determined accurately. The results are shown in Fig. 4a. As not all complexes are easily soluble in hexane, the same process can be used to reference to DMA. In almost every case, the negative values in Figure 4a correspond to referencing against hexane, and positive values to DMA. As with the Bellamy plots for individual complexes, this plot using relative wavenumbers also shows a good grouping of data points to the diagonal, and the data referenced to hexane and DMA correspond to the same general trend, indicating that in practice, both referencing methods are similarly reliable. The plot also provides a comparison of the overall range of solvent-differentiating powers of these complexes. In all the cases examined, we have used THF as one of the solvents, and referencing against THF also produces a good means to compare the Bellamy plots (Fig. 4b), and allows all the data in Table 1 to be placed on the same plot. The results in Fig. 4 show that the complexes mostly show similar responses, though they do not fit to exactly the same line. The 1,4-dimethoxy complex **3** in particular is significantly different from the other iron complexes (the slope of the line is lower). More notably, the response measured for the manganese complex **15** stands clearly apart from the main body of data. For the iron, chromium and cobalt complexes, the vibrational bands measured are symmetric and antisymmetric vibrational modes of the same $\text{M}(\text{CO})_3$ unit (or $\text{M}_2(\text{CO})_6$ in the case of cobalt), but in the $\text{Mn}(\text{CO})(\text{NO})\text{PPh}_3$ complex, the data is taken from the separate CO and NO bands. The degree of vibrational coupling between the $\nu(\text{CO})$ and $\nu(\text{NO})$ modes will be very much less than that within an $\text{M}(\text{CO})_3$ unit, and the data obtained from this carbonyl(nitrosyl)metal complex lies well off the regression lines in Fig. 4. For this reason, and because of complications with interference from the solvent background in polar solvents, the solvent-induced shifts for $\text{Mn}(\text{CO})(\text{NO})\text{PPh}_3$ were not studied further.

The degree of differentiation of environments demonstrated by each complex was judged in our original study [8] by calculation of the diagonal separation (Δ) of the extreme points on the plot, corresponding to polar solvents such as dimethylformamide (DMF) and dimethylacetamide (DMA) and non-polar solvents such as hexane and cyclohexane. The parameter (Δ) was defined as:

$$\Delta = \{[\nu_s(\text{hexane}) - \nu_s(\text{DMA})]^2 + [\nu_{as}(\text{hexane}) - \nu_{as}(\text{DMA})]^2\}^{1/2} \quad (1)$$

in cases where the vibrational signals for measurements in hexane and DMA lie at the extremes of the Bellamy plot.

Data presented in Table 1 now shows that this property is valuable for the comparison of a wide selection of organometallic complexes (Fig. 2, **1-5** and **12-15**) in solution, and also that for a given solvent, a wide variety of band positions can be obtained by choice of suitable carbonylmetal complexes. For each complex, the positions of points for measurements in hexane or cyclohexane always appear close together at the upper end of the diagonal line in the Bellamy plot, and those for DMA and DMF at the lower end of the line.

Table 1.

Solvent	Complex	Observed IR stretching modes		Data from Bellamy plots		Relative peak positions		Ref.
		ν_s Peak Position	ν_{as} peak position	$\nu_{R(\text{solvent})}$	ratio $\nu_{R(\text{solvent})}$ and $\nu_{R(\text{DMA})}$	$\nu_s(\text{rel : hexane})$	$\nu_{as}(\text{rel : DMA})$	
(note a)	(note b)	(cm ⁻¹)	(cm ⁻¹)	(cm ⁻¹)		(rel. cm ⁻¹)	(rel. cm ⁻¹)	(note d,e)
1	1	2043.8	1973.0	0.00		0.0	0.0	[8] ^d
1	2	2047.0	1975.8	0.00		0.0	0.0	
1	3	2040.7	1968.8	0.00		0.0	0.0	
1	4	2047.4	1975.8	0.00		0.0	0.0	[8] ^e
1	12	1991.3	1930.5	0.00		0.0	0.0	[8] ^e
1	13	1973.2	1901.2	0.00		0.0	0.0	[8] ^e
1	14'	2097.6	2058.1	0.00		0.0	0.0	[8] ^e
1	14''	2097.6	2031.0	0.00		0.0	0.0	[8] ^e
1	15	1955.4	1703.0	0.00		0.0	0.0	
2	1	2042.5	1971.0	2.39	0.12	-1.3	-2.0	[8] ^d
2	2	2046.0	1974.0	2.06	0.12	-1.0	-1.8	
3	3	2039.6	1967.7	1.56	0.07	-1.1	-1.1	
4	3	2037.4	1963.1	6.59	0.31	-3.3	-5.7	
5	3	2037.0	1963.1	6.80	0.32	-3.7	-5.7	
6	1	2040.8	1967.5	6.26	0.33	-3.0	-5.5	[8] ^d
6	2	2044.0	1971.8	5.00	0.29	-3.0	-4.0	
7	1	2040.3	1966.8	7.12	0.37	-3.5	-6.2	[8] ^d
7	2	2044.0	1971.3	5.41	0.31	-3.0	-4.5	
7	3	2036.7	1962.3	7.63	0.36	-4.0	-6.5	
7	13	1965.5	1889.4	14.10	0.37	-7.7	-11.8	[8] ^e
8	1	2037.8	1963.8	10.98	0.57	-6.0	-9.2	[8] ^d
8	2	2042.3	1968.0	9.11	0.53	-4.7	-7.8	
8	3	2035.7	1958.1	11.81	0.55	-5.0	-10.7	
8	13	1961.7	1881.0	23.20	0.60	-11.5	-20.2	[8] ^e
9	1	2037.8	1963.0	11.66	0.61	-6.0	-10.0	[8] ^d
9	2	2041.0	1967.0	10.65	0.62	-6.0	-8.8	
9	3	2034.6	1958.0	12.40	0.58	-6.1	-10.8	
10	1	2038.0	1962.8	11.73	0.61	-5.8	-10.2	[8] ^d
10	2	2042.0	1966.3	10.74	0.62	-5.0	-9.5	
10	3	2034.5	1959.0	11.60	0.54	-6.2	-9.8	
11	1	2036.8	1962.0	13.04	0.68	-7.0	-11.0	[8] ^d
11	2	2040.8	1966.5	11.18	0.65	-6.2	-9.3	
11	3	2032.8	1956.4	14.70	0.69	-7.9	-12.4	
11	4	2041.2	1969.5	8.84	0.62	-6.2	-6.3	[8] ^e
11	12	1975.3	1903.8	31.1	0.74	-16.0	-26.7	[8] ^e
11	13	1959.3	1878.2	26.9	0.70	-13.9	-23.0	[8] ^e
11	14'	2093.0	2052.5	7.25	0.81	-4.6	-5.6	[8] ^e
11	14''	2093.0	2025.3	7.32	0.71	-4.6	-5.7	[8] ^e
11	15	1942.3	1695.8	14.95		-13.1	-7.2	
12	1	2036.8	1960.8	14.07	0.74	-6.5	-12.2	[8] ^d
12	2	2041.3	1965.8	11.51	0.67	-5.7	-10.0	
12	3	2032.8	1956.4	14.70	0.69	-7.9	-12.4	
13	1	2037.0	1961.3	13.53	0.71	-6.8	-11.7	[8] ^d
13	2	2041.3	1965.5	11.77	0.68	-5.7	-10.3	

14	1	2037.3	1960.8	13.82	0.72	-6.5	-12.2	[8] ^d
14	2	2041.5	1965.0	12.12	0.70	-5.5	-10.8	
15	1	2034.5	1956.8	18.68	0.98	-9.3	-16.2	[8] ^d
15	2	2038.5	1961.0	17.07	0.99	-8.5	-14.8	
16	1	2033.3	1957.0	19.14	1.00	-10.5	-16.0	[8] ^d
16	2	2038.0	1961.0	17.32	1.00	-9.0	-14.8	
16	3	2028.6	1951.2	21.36	1.00	-12.1	-17.6	
16	4	2038.2	1964.8	14.34	1.00	-9.2	-11.0	[8] ^e
16	12	1970.3	1893.8	42.30	1.00	-21.0	-36.7	[8] ^e
16	13	1953.5	1868.1	38.50	1.00	-19.7	-33.1	[8] ^e
16	14'	2091.8	2051.3	8.94	1.00	-5.8	-6.8	[8] ^e
16	14''	2091.8	2022.5	10.29	1.00	-5.8	-8.5	[8] ^e
16	15	(note f)	(note f)					
16	5	2033.3	1957.5	0.00		0.0	0.0	
15	5	2034.5	1957.4	1.20	0.11	1.2	-0.1	
12	5	2037.3	1962.1	6.10	0.54	4.0	4.6	
11	5	2036.5	1963.0	6.40	0.57	3.2	5.5	
8	5	2037.9	1963.9	7.90	0.70	4.6	6.4	
7	5	2039.3	1967.0	11.20	1.00	6.0	9.5	
6	5	2038.5	1966.0	10.00	0.89	5.2	8.5	
1	5	(note g)	(note g)					

^a key to solvent codes: 1: hexane; 2: cyclohexane; 3: dodecane; 4: propan-1-ol; 5: butan-1-ol; 6: octan-1-ol; 7: diethyl ether; 8: ethyl acetate; 9: toluene; 10: dichloromethane; 11: tetrahydrofuran; 12: acetone (propan-2-one); 13: acetic anhydride; 14: acetonitrile; 15: dimethylformamide; 16: dimethylacetamide.

^b for key to structures of complexes, see Figure 2. For complex **14**, **14'** indicates that the higher wavenumber \square_{asym} band is listed, and **14''** indicates the lower wavenumber \square_{asym} band.

^c \square and relative peak positions are tabulated relative to hexane in all cases except the organometallic naringenin derivative which was insufficiently soluble in hexane; values relative to DMA, or THF can be calculated from the tabulated data following the same procedure by substitution of an alternative choice of reference solvent in equation (2).

^d data presented in graphical form in the publication cited.

^e data presented only as a range of values in the publication cited.

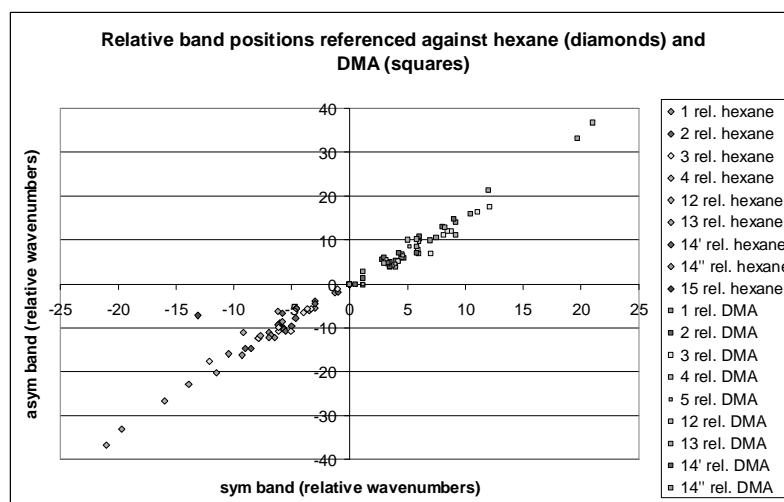
^f vibrational bands of the NO ligand in DMA were obscured by the solvent background spectrum.

^g insufficiently soluble in hexane.

However, for solvents of intermediate types there is a degree of variation in rank order in which they appear on the diagonal of a Bellamy plot. Simple attempts to relate this property to typical physical measures of the nature of each solvent quickly showed that such issues are far from straightforward. Plots of the position of IR bands of **1** against parameters [21-24] such as electric dipole moment, dielectric constant, polarity index, or molecular polarizability showed substantial scatter and poor correlations to a linear plot. Even in the best case (polarity index [24]), the order of solvents on that plot did not correspond to the order in the Bellamy plot [8] for **1**, and different complexes produced different orders of solvents when ranked in terms of their effect on the IR vibrational modes. The variation in rank order of solvents for different complexes reflects the complexity of factors that influence the vibrational properties of carbonylmetal complexes in solution. This variation can be quantified by calculating for each point a diagonal separation from the fixed point of a reference solvent, on the same principle as the calculation used [8] to determine Δ . We define this parameter $\Delta_{\text{R(solvent)}}$. Hexane was again chosen as the preferred reference solvent because of the narrow nature of the IR bands in hydrocarbon solution. $\Delta_{\text{R(solvent)}}$ is calculated as shown in equation 2.

$$\Delta_{\text{R(solvent)}} = \{[v_{\text{s}}(\text{hexane}) - v_{\text{s}}(\text{solvent})]^2 + [v_{\text{as}}(\text{hexane}) - v_{\text{as}}(\text{solvent})]^2\}^{1/2} \quad (2)$$

(a)



(b)

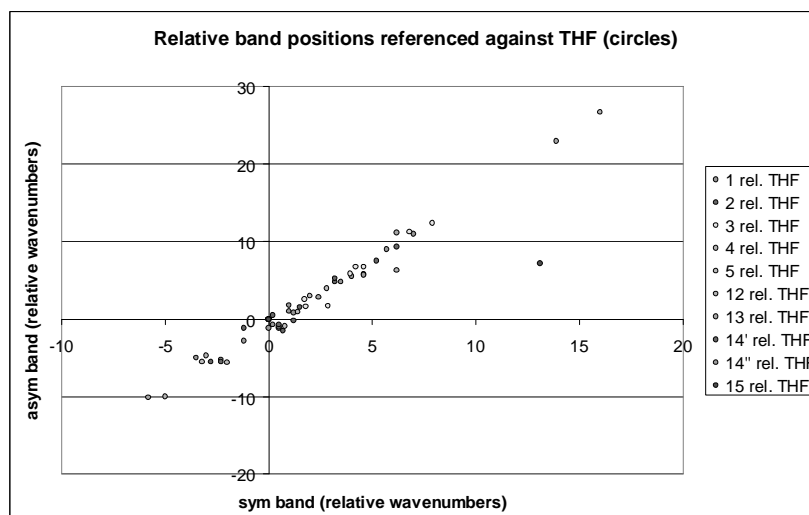


Fig. 4. Comparison of complexes **1**, **2**, **3**, **4**, **5**, **12**, **13**, **14**, and **15** by means of Bellamy plots of relative peak positions, calculated relative to: (a) hexane (points marked as diamonds) and DMA (points marked as squares); (b) THF (points marked as circles).

The long-term objective of our work is to apply these procedures to address biological issues [17, 25-27], so the differentiation of environment-induced shifts in the IR spectra is of particular importance. The ends of the diagonal in Bellamy plots such as Fig. 4b, or the solution data section (points a-j) in Fig. 3b, for example, correspond to hydrophilic and hydrophobic environments. However, the more subtle factors that influence the relative positions of bands in different solvents will ultimately prove more important to address specific biological issues, so we have examined in more detail, the factors that contribute to high discriminatory effects. The simple calculation of Δ [8] is not on its own an adequate guide, since a large variation of the ordering of the peaks, when the spectra of one complex are compared to another, can be just as powerful as a means of obtaining discrimination in a multi-carbonylmetal procedure. Using the data presented in Table 1, values for differences in normalised Δ_R values (Δ_N) have been calculated (equation 3) using the ratio of $\Delta_{R(\text{solvent})}$ and $\Delta_{R(\text{DMA})}$ for each solvent.

$$\Delta_{N(\text{complex } X)} = \frac{\Delta_{R(\text{solvent } n)(\text{complex } X)} - \Delta_{R(\text{solvent } m)(\text{complex } X)}}{\Delta_{R(\text{DMA})(\text{complex } X)}} \quad (3)$$

The term Δ_N corresponds to the normalised diagonal separation of two data points on the Bellamy plot, and so allows results from different complexes to be compared on a common basis. We have used the normalised differential responses from equation 3 to compare the two methoxydiene complexes **1** and **2**, to identify cases where the compounds behave differently in terms of their responses to a pair of solvents. The comparison was made by determining the ratio (equation 4) of $\Delta_{N(\text{complex } 1)}$ and $\Delta_{N(\text{complex } 2)}$ for the two complexes.

$$\frac{\Delta_{N(\text{complex } 1)}}{\Delta_{N(\text{complex } 2)}} = \frac{\Delta_{R(\text{solvent } n)(\text{complex } 1)} - \Delta_{R(\text{solvent } m)(\text{complex } 1)}}{\Delta_{R(\text{solvent } n)(\text{complex } 2)} - \Delta_{R(\text{solvent } m)(\text{complex } 2)}} \times \frac{\Delta_{R(\text{DMA})(\text{complex } 2)}}{\Delta_{R(\text{DMA})(\text{complex } 1)}} \quad (4)$$

The results obtained for two methoxydiene complexes **1** and **2** are displayed on the z axis of Fig. 5a in terms of percentages. Axes x and y correspond to the list of different solvents, and each point on the xy plane identifies a pair of solvents. Positive or negative values in the z direction correspond to good complementary responses to the pair of solvents identified at that position on axes x and y, and thus a high level of discrimination. In this case, the large positive values near the centre of the plot correspond to comparisons of effects by solvents such as toluene, dichloromethane and tetrahydrofuran. The most significant negative values arise from comparing acetone and acetic anhydride. The mean value of these normalised differential responses was 1.05. Fig. 5a is presented to illustrate the principle of application of this type of plot, and the method is employed in Section 3.4 to define the properties of a multi-carbonylmetal measurement approach on the optrode.

3.2. Studies with adsorbed organometalcarbonyl complexes

By supporting our organometallic sensor molecules on solid phases, we hope to gain in terms of convenience of use, and by-pass problems with limitations of applicability because of inadequate solubility. It is possible to envisage simply adding the sensor preparation to a solution of the analyte, measuring the spectrum, and filtering to recover the sensor. This is an attractive procedure for routine application, and will be an important step towards the application of our method to biological samples [17, 25-27]. However, the solvents and analytes must gain intimate contact with the organometallic complex to induce an effect, and problems with efficient “wetting” of the surface, or loss of access to the active component within the structure introduced to attach it to the support, were concerns at the outset. To make an initial assessment to determine that the solvent-response properties in solution can be duplicated with supported compounds, a simple test was performed by adsorbing the carbonyliron complexes onto 40 mesh silica with an average particle size 5-15 μm and a surface area 600 $\text{m}^2 \text{g}^{-1}$ by dissolving in dichloromethane, adding the silica, and evaporating. The coated silica gel was measured using DRIFT spectroscopy and the spectrum was ratioed against the DRIFT spectrum of untreated silica gel. Using the 1,4-dimethoxy-substituted complex **3**, the spectra obtained showed peaks for the $\nu_s(\text{CO})$ and $\nu_{as}(\text{CO})$ modes shifted to 2047 and 1977 cm^{-1} respectively. This additional point (entry k) was added to the Bellamy plot of $\nu(\text{CO})$ frequencies in solution (Fig. 3b) illustrate the effect of adsorption on silica gel. In this case, the adsorbed complex **3** shows a correlation with the solvent spectra on the Bellamy plot by lying on the regression line, however, it is also shifted to much higher wavenumbers due to the silica gel/complex interaction. Repetition of this procedure at three different loadings produced progressive increases in intensity of the shifted bands at 0.2, 0.5 and 5.0 % w/w levels, while band positions and widths remained comparable (Fig. 6a). When these samples were aged,

new bands appeared at higher wavenumbers. Similar results were obtained with the 1-methoxy-substituted complex **1**, which was stable on silica for many hours and gave shifted bands at 2046 and 1976 cm^{-1} . Although the intensity of bands decreased slowly with time, new signals from carbonylmetal decomposition products were not encountered in this case. Fig. 6b shows results from aging experiments with the 1-methoxy-substituted complex **1** conducted over a period of three weeks.

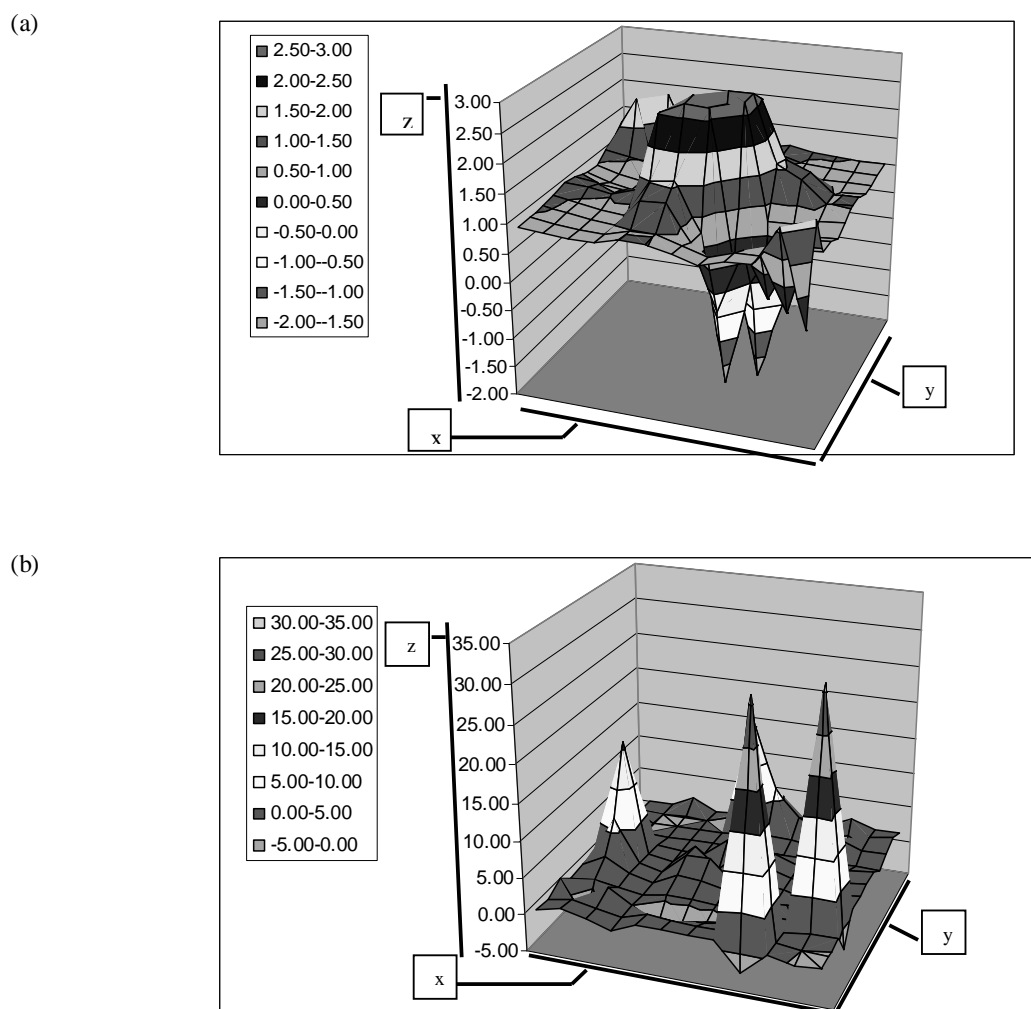


Fig. 5. Pairwise comparison of responses complexes in different solvents. (a) complexes **1** and **2** with solvents listed along the x axis from left to right in the order: hexane, cyclohexane, 1-octanol, diethylether, toluene, dichloromethane, tetrahydrofuran, acetone, acetonitrile, dimethylformamide, dimethylacetamide. (Solvents are listed along the y axis from front to back in the order: dimethylacetamide, dimethylformamide, acetonitrile, acetone, tetrahydrofuran, dichloromethane, toluene, diethylether, 1-octanol, cyclohexane, hexane.); (b) immobilised samples prepared [14] from complexes **22** and **24** with solvents listed along the x axis from left to right in the order: hexane, dodecane, chloroform, methanol, dichloromethane, diethylether, acetonitrile, acetone, dioxane, tetrahydrofuran, dimethylformamide, dimethylsulfoxide. (Solvents are listed along the y axis from front to back in the order: dimethylsulfoxide, dimethylacetamide, tetrahydrofuran, dioxane, acetone, acetonitrile, diethylether, dichloromethane, methanol, dodecane, hexane).

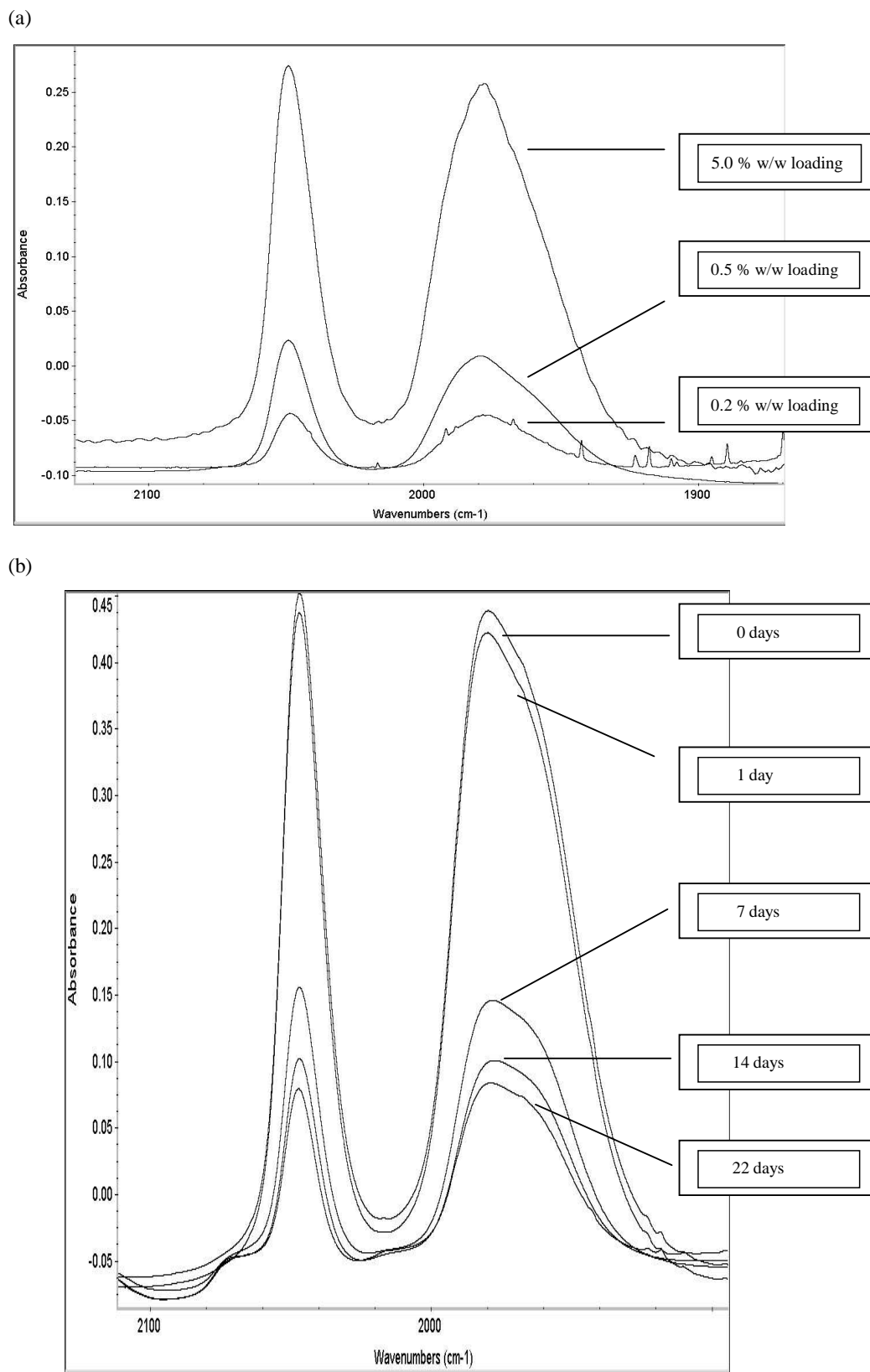


Fig. 6. Tricarbonyl(η^4 -cyclohexadiene)iron complexes adsorbed onto silica. a) FTIR spectrum of 0.2, 0.5 and 5.0 % w/w tricarbonyl(η^4 -1,4-dimethoxycyclohexadiene)iron(0) (3) coated silica gel measured using DRIFTS; b) DRIFT spectra of tricarbonyl(η^4 -1-methoxycyclohexadiene)iron(0) (1) after 0, 1, 7, 14 and 28 days of adsorption onto silica.

This supported complex was then examined in a range of solvents using a horizontal ATR accessory in the sample well of the FTIR spectrometer, by simply spreading the loaded silica onto the ATR crystal and wetting with each solvent. Better quality spectra were obtained using a two-compartment liquid sample cell constructed employing a PTFE semipermeable membrane to separate the silica from the bulk solvent. This cell could be filled and emptied in the same manner as a standard solution cell, and was employed to make a series of IR measurements with binary mixtures of dichloromethane and hexane. The results showed that the $\nu(\text{CO})$ bands of the carbonylmetal moiety shifted reversibly with respect to binary solvent compositions establishing that the two-compartment cell allowed sensing interactions of silica supported organometalcarbonyl sensors to be detected. However, as the experiment progressed, the organometalcarbonyl complex was gradually washed off the silica surface, causing the $\nu(\text{CO})$ band intensities to decrease progressively over a series of experiments. None-the-less, useful spectra were obtained, and treatment of the data by the PCA method produced a factor score plot that illustrated the response of the system to different solvent ratios. This series of experiments showed that with the correct choice of organometallic complex, good stability and good responses to environment effects could be obtained on the silica support.

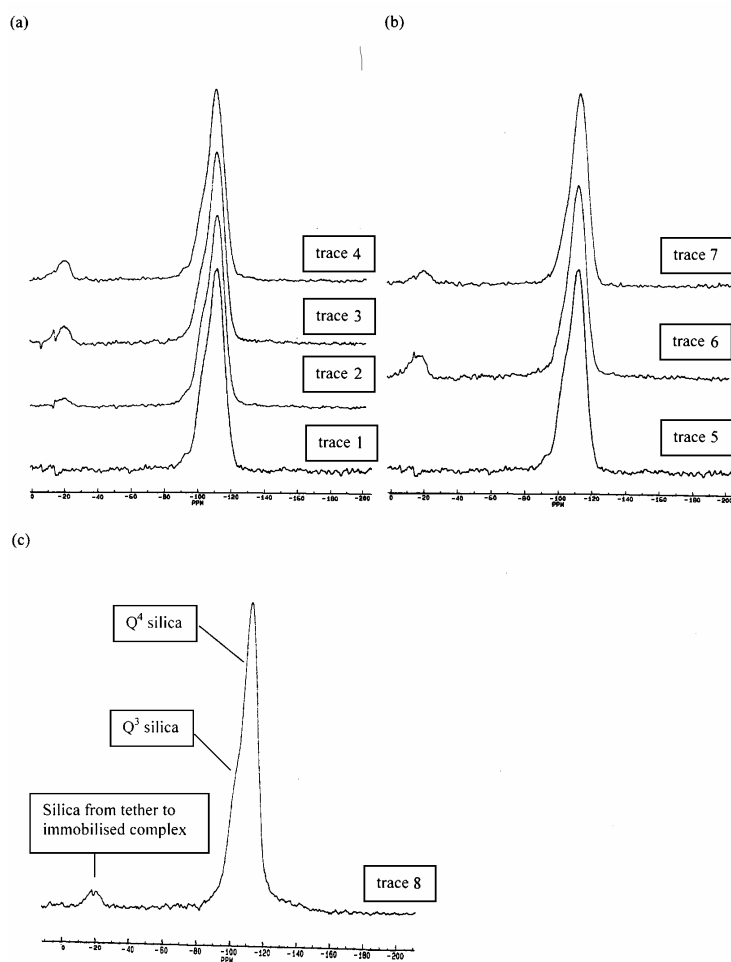


Fig. 7. ^{29}Si NMR spectra of complex **22** immobilised on 40 mesh silica and silica nanoparticles. (a) 40 mesh silica: trace 1: untreated silica; trace 2: after first treatment with tricarbonyl[5-(η^4 -cyclohexadien-1-yl)iron(0)] $\text{HNCH}_2\text{CH}_2\text{CH}_2\text{SiMe}(\text{OEt})_2$; trace 3: after second treatment; trace 4: after third treatment. (b) 40 mesh silica: trace 5: untreated silica; trace 6: after treatment with $\text{H}_2\text{NCH}_2\text{CH}_2\text{CH}_2\text{SiMe}(\text{OEt})_2$; trace 7: after subsequent reaction with the tricarbonyl(cyclohexadienyl)iron(1+) complex. (c) silica nanoparticles: trace 8: after treatment with tricarbonyl [5-(η^4 -cyclohexadien-1-yl)iron(0)] $\text{HNCH}_2\text{CH}_2\text{CH}_2\text{SiMe}(\text{OEt})_2$.

3.3. Covalent attachment of organometalcarbonyl complexes to silica

We turned next to the issue of covalent attachment of the organometallic to the silica surface. A widely used approach [28] to achieve attachment to silica employs a 1-amino-3-silylalkyl group, and we have already described the application of the methodology with tricarbonyliron complexes [12, 13]. The method is convenient because the nucleophilic amino group can be used in reactions with cationic tricarbonyl(η^5 -cyclohexadienyl)iron electrophiles. In this way, a wide selection of substituted organometallic complexes can be introduced by the same procedure, and we describe here the extension of our initial results with tricarbonyliron and dicarbonyl(triphenylphosphine)iron complexes of the unsubstituted cyclohexa-1,3-diene ligand [12, 13] to three substituted examples (**16-18**: $R^1 = \text{CO}_2\text{Me}$, $R^2 = \text{H}$; $R^1 = \text{H}$, $R^2 = \text{C}_6\text{H}_3\text{O}_2\text{CH}_2$; $R^1 = \text{H}$, $R^2 = \text{CH}_2\text{CH}_2\text{CO}_2\text{Me}$). Previously we have used [13] atomic absorption (AA) spectroscopy to estimate the quantity of iron complex attached to the surface of the silica by determining iron concentrations. Conventional C, H and N microanalysis can also give a useful guide (Table 2). Untreated silica was found as expected to have a low carbon and nitrogen content. Washing the silica with the solvents used for the immobilisation of the organometallic complex, and then drying, was found to leave some residual hydrocarbon on the silica. After addition of the immobilised organometalcarbonyl complex, however, greater levels of carbon and hydrogen were found, and nitrogen could also be detected. The nitrogen content was ascribed to the presence of the nitrogen atoms attaching the aminosilylalkyl tethers to the cyclohexadiene complexes, and so gives an estimate of the quantity of immobilised material.

Table 2.

Estimation of immobilisation of tricarbonyl[5-(2-methoxy- η^4 -cyclohexadien-1-yl)iron(0)]HNCH ₂ CH ₂ CH ₂ SiMe(O-) ₂ 20 on silica ^a by microanalysis.		
	Untreated silica ^a	Treated silica
C (%)	<0.3	6.08
H (%)	0.49 ^b	1.03 ^c
N (%)	<0.3	0.53 ^d
Observed (N:C) ratio	not calculated	0.087 ^e
Theoretical (N:C) ratio		0.083 ^f
^a 60 mesh silica.		
^b the hydrogen content is ascribed to surface OH groups (silanol and adsorbed water).		
^c because of the unknown contribution from the residual silanol hydrogen content, the H analysis does not perform well as a measure of immobilised organometallic.		
^d the nitrogen content is ascribed to the presence of the nitrogen atom attaching the tether to the cyclohexadiene complex.		
^e close to the theoretical value calculated from the carbon/nitrogen content of the reagent (excluding the ethyl groups of the SiMe(OEt) portion).		
^f C ₁₄ H ₁₉ FeNO ₄ Si requires C 48.1% H 5.5% Fe 16.0% N 4.0% O 18.3% Si 8.0%.		

Solid state ²⁹Si NMR spectroscopy, however, has now been used to provide a far more direct and complementary confirmation of the covalent attachment of the metal complex by the use of the aminosilylalkyl tether. The spectrum of untreated silica (Fig. 7a, trace 1) displays the well known [29] pair of overlapping signals at about -100 ppm. The main signal at -110 ppm corresponds to ²⁹Si within the bulk of the Si-O matrix (the majority of these sites will have four Si-O-Si bonds to each silicon atom). This position in the silica is referred to as Q⁴. On the surface, a typical silicon atom differs from Q⁴ by having one silanol SiOH silicon-oxygen bond. This Q³ position has a slightly different ²⁹Si chemical shift, and can be seen as the shoulder at -103 - -106 ppm on the side of the -110 ppm Q⁴ band. Derivatisation of the silica with the organometallic reagent was found to introduce

an additional band at -19 ppm when the product was investigated by ^{29}Si MAS NMR (Fig. 7a, trace 2). Repeated treatment of the same sample of silica with the organometallic reagent caused a progressive increase in the intensity of the new signal at -19 ppm (Fig. 7a, traces 3 and 4). It can also be seen that the Q^3 band decreased in intensity as the extent of surface attachment of the organometallic complex was increased. As the derivatisation procedure works by reaction of the $\text{SiMe}(\text{OEt})_2$ group on the reagent with surface silanol groups on the silica, the proportion of silanol groups to bulk silica should be decreased after attachment of the organometallic. This is consistent with the reduction of intensity of the Q^3 band, which indicates that substantial levels of surface coverage are achieved in this way. The Q^3 shoulder at -103 - -106 ppm is considerably reduced in the spectrum (Fig. 7a, trace 4) obtained from the sample that carries the greatest loading of carbonyliron complex. This sample also has the most intense metal carbonyl peaks in its IR spectrum and the least intense SiOH bands (see below, and Fig. 8). The $\text{H}_2\text{NCH}_2\text{CH}_2\text{CH}_2\text{SiMe}(\text{OEt})_2$ itself was also attached to the silica by the same method. In this case, a low-field resonance was again observed. The Q^3 band was reduced in height, and in Fig. 7b (trace 6) can hardly be detected on the side of the main Q^4 band. This sample of silica carries surface aminoalkyl groups, and was treated with the electrophilic tricarbonyl(η^5 -cyclohexadienyl)iron(1+) complex. Although the product of the initial reaction with $\text{H}_2\text{NCH}_2\text{CH}_2\text{CH}_2\text{SiMe}(\text{OEt})_2$ showed the most intense band at -20 ppm, after addition of the tricarbonyliron group the band observed was found to be only of intermediate height (Fig. 7b, trace 7). It was clear from these experiments that although both reaction sequences afforded the same type of covalently attached supported organometallic complex, addition of the tether first to the tricarbonyl(η^5 -cyclohexadienyl)iron(1+) complex and then attachment to silica gave the simplest method to achieve high loadings. These experiments show the utility of ^{29}Si MAS NMR as a tool to confirm successful attachment of the organometallic complex, and the ^{29}Si NMR results also confirm our original assignments [12-14] of the nature of the covalently attached species.

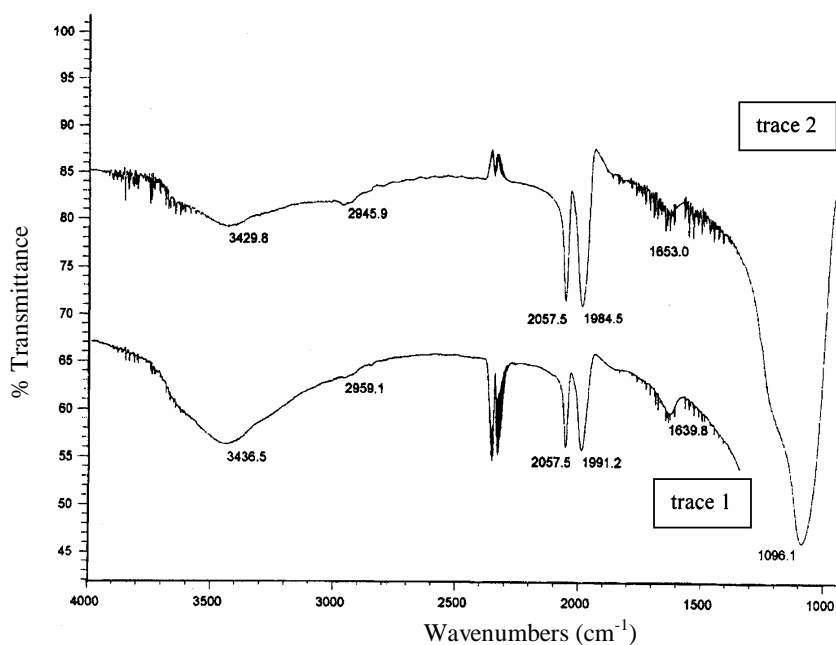


Fig. 8. FTIR spectra of complex **22** immobilised on 40 mesh silica and pressed into a KBr disk. Trace 1: after first treatment with tricarbonyl [5- (η^4 -cyclohexadien-1-yl) iron(0)] $\text{HNCH}_2\text{CH}_2\text{CH}_2\text{SiMe}(\text{OEt})_2$; trace 2: after third treatment.

In the course of this work, FTIR in KBr disks and DRIFT spectra were also recorded and evaluated as means of checking the surface loading. IR bands for the attached carbonyliron complex could be clearly detected, and their intensities could be estimated by measurement of ratios of peak

intensities, using a major peak at 1090-1096 cm^{-1} in the KBr spectrum or 840-850 cm^{-1} in the DRIFT spectrum of underivatised silica as reference peaks. The samples of silica obtained by repeated treatment with the tricarbonyl[5-(η^4 -cyclohexadien-1-yl)iron(0)]HNCH₂CH₂CH₂SiMe(OEt)₂ reagent provided an opportunity to check the suitability of these procedures, and the loading of iron in each sample was determined by atomic absorption spectroscopy (Method A). Fig. 9 shows the satisfactory correspondence between the ratios of Kubelka-Munk values for ν_{sym} at 2057.5 cm^{-1} and the reference band, and the iron present. AA analysis of iron was also performed on the underivatised silica, and a small quantity of background iron was detected. This background value was subtracted from the observed levels before conversion by use of a calibration curve to give a measure of the iron added in the experiment. Pressing the derivatised silica sample into KBr disks allows transmission spectra to be recorded, but we found that conversion of the peak heights into absorbance units [absorbance = $-\log_{10}(\text{transmission})$] and calculating ratios against the large reference peak at 1096 cm^{-1} did not prove to a good quantitative procedure. However, transmission IR spectra did give good qualitative information and the examples in Fig. 8 show that after the sequence of repeated additions of tricarbonyl[5-(η^4 -cyclohexadien-1-yl)iron(0)]HNCH₂CH₂CH₂SiMe(OEt)₂ the IR bands of the carbonylmetal complex have increased, and the surface silanol groups have decreased. This is consistent with the effects seen in the ²⁹Si NMR and supports the interpretation of the observed reduction in intensity of the Q³ band. As one would hope, the IR spectrum of the silica treated only with H₂NCH₂CH₂CH₂SiMe(OEt)₂ contained no bands in the carbonylmetal stretching region around 2000 cm^{-1} , and when the product was reacted with tricarbonyl(η^5 -cyclohexadienyl)iron(1+), the typical Fe-CO vibrational bands reappeared. The availability of the AA data discussed above allows our interpretation of the ²⁹Si NMR results to be checked. Integrations of the signal at -19 ppm and the entire overlapping signal for the Q³ and Q⁴ silica can be expected to give a guide to loadings. The Q³ contribution to the -100 ppm signal decreases as the -19 ppm signal increases, but the Q³ environment is converted into a Q⁴ position in the reaction, so the Q⁴ band should be increased. The ratio of integrations measured at -19 and -100 ppm, however, was found to overestimate the loading at high loadings. Differences in relative relaxation times, or contributions from inaccurate measurement of the baseline at low loadings may be the source of this effect. This ratio is plotted in Fig. 8 against concentrations of iron obtained by AA (Method B). The changing Q³:Q⁴ ratio also leads to a degree of variation in the apparent position of the maximum of the Q⁴ signal on the ppm scale.

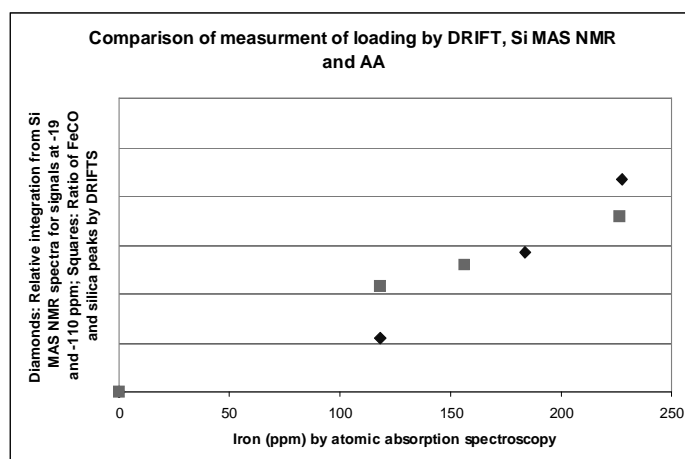
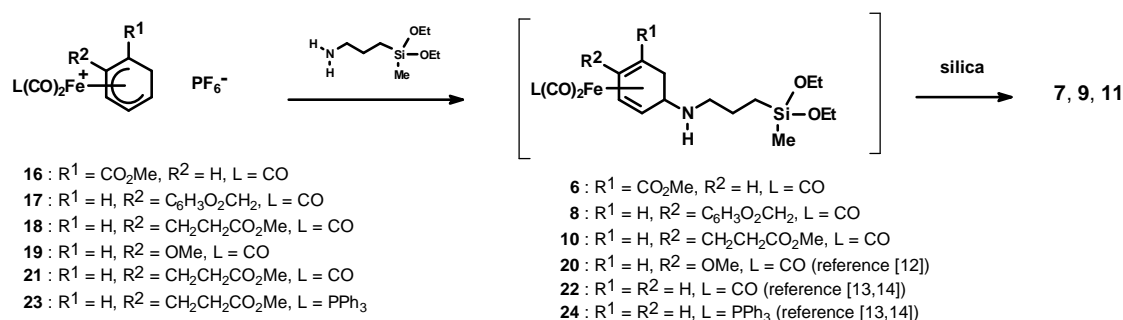


Fig. 9. Plots of loading determined by DRIFTS (squares: vertical scale 1 per division) and ²⁹SiNMR (diamonds: vertical scale 2 per division) after immobilisation of complex **22** on 40 mesh silica.

Atomic absorption spectroscopy remains the best way to quantify the surface-bound metal complex, but DRIFT spectra can also give a reasonable guide to relative loadings. The results described here also show that ²⁹Si solid state NMR spectroscopy is a powerful tool for direct study of the tricarbonyliron complexes on the silica surface.

The procedures established in this way were now used to attach three substituted cyclohexadiene complexes to 40 mesh silica (Scheme 1), by first reacting the electrophilic tricarbonyl(η^5 -cyclohexadienyl)iron(1+) complexes examples **16-18** ($R^1 = \text{CO}_2\text{Me}$, $R^2 = \text{H}$; $R^1 = \text{H}$, $R^2 = \text{C}_6\text{H}_3\text{O}_2\text{CH}_2$; $R^1 = \text{H}$, $R^2 = \text{CH}_2\text{CH}_2\text{CO}_2\text{Me}$) with $\text{H}_2\text{NCH}_2\text{CH}_2\text{CH}_2\text{SiMe}(\text{OEt})_2$, and then adding the product to the silica. These methods were also used with ~ 7 nm silica nanoparticles to attach complex **22** [13, 14], and examination of the nanoparticles by ^{29}Si NMR gave similar results to those described above (Figs. 7c, trace 8), with the main Q^4 band appearing at -112 ppm and the Q^3 shoulder as before between -103 and -106 ppm. The ^{29}Si resonance for the bound organometallic compound was again found at -19 ppm.

Scheme 1



3.4. FTIR studies of covalently attached organometalcarbonyl complexes by ATR and optode-ATR procedures

The $\nu(\text{CO})$ modes of the substituted immobilised complexes **7**, **9** and **11** were studied in eight different environments to determine their responses. These environments were diethylether, dichloromethane, methanol, hexane, acetonitrile, toluene, acetone and water. The baseline ATR accessory was used for recording the spectra. A 1 % w/w suspension of the individual complexes was made up in methanol and the ATR accessory was dipped into the suspension seven or eight times until a matt finish was observed on the ZnSe element. A spectrum of the immobilized complex was then recorded in each of the eight solvents and the results plotted in a Bellamy plot (Fig. 10).

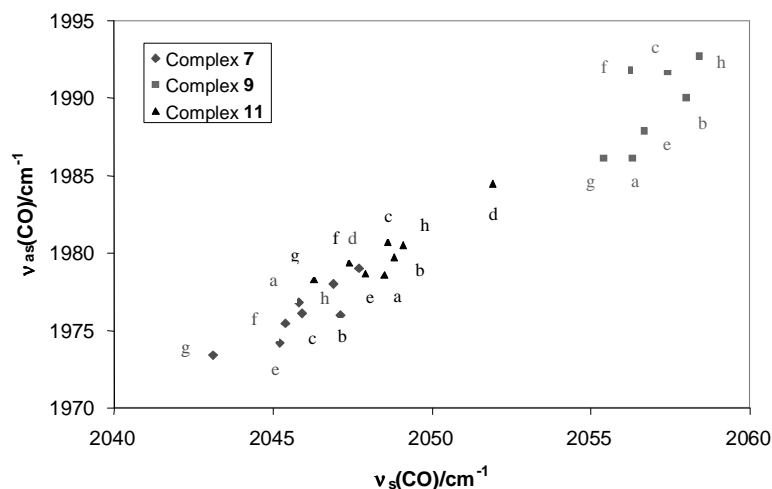


Fig 10. Bellamy plot of $\nu_s(\text{CO})$ against $\nu_{\text{as}}(\text{CO})$ of immobilised complexes **7**, **9** and **11** in eight different solvent environments; a = diethylether, b = dichloromethane, c = methanol, d = hexane, e = acetonitrile, f = toluene, g = acetone, g = water.

Finally, a study was made of the responses to changing solvent environments of dicarbonyl[5-(η^4 -cyclohexadien-1-yl)(triphenylphosphine)iron(0)]HNCH₂CH₂CH₂SiMe(O-)₂] (**24**) on silica nanoparticles supported on the optrode device. Compared to our earlier investigation [14] of the tricarbonyl[5-(η^4 -cyclohexadien-1-yl)iron(0)]HNCH₂CH₂CH₂SiMe(O-)₂] example (immobilised **22**), a greater degree of scatter was observed in the dicarbonylphosphine case (Fig. 11). There is also very considerable variation in the rank orders of solvents in the two sets of data. The methods described in Section 3.1 were now put into practice to characterise the properties of the dual probe complexes on the optrode device by comparing normalised differential response ratios for two complexes for all the combinations of pairs of solvents. The results are displayed as displacements in terms of percentages on the z axis of Fig. 5b. The mean value of the normalised differential responses measured in this way with the immobilised complex on silica was 1.56, but this contains some very large positive values, and so does not clearly reflect the position of the xy plane in Figure 5b, which is considerably lower than that in Fig. 5a for the results obtained in solution. To calculate the data in Fig. 5b, comparisons with ethyl acetate were omitted because the data for ethyl acetate fell outside the hexane-DMA span of the diagonal on the Bellamy plot. There are several significant differences between the results in Fig. 5a and Fig. 5b. For example, the dichloromethane / tetrahydrofuran comparison which gave a significant positive value in Fig. 5a produced a negative value in Fig. 5b. Introduction of new solvents (chloroform and dioxane, which were not used in the solution experiments because of their toxicity) into the experiments with the optrode gave the very large positive values. We have commented earlier [14] on the anomalous effect of water in the examination of solvents using the optrode. As a highly polar solvent, water might be expected to appear beyond DMF on the Bellamy plot [14] for complex **22**, but instead lies beyond hexane, and in Fig. 11, the entry for water (i) takes an intermediate position near the chlorinated solvents and ethyl acetate. Some of the differences between the plots in Fig. 5 are similarly likely to arise from such special properties of the supported organometallic complexes, however, a contribution from effects from the presence of the phosphine ligand in immobilised **24** cannot be ruled out.

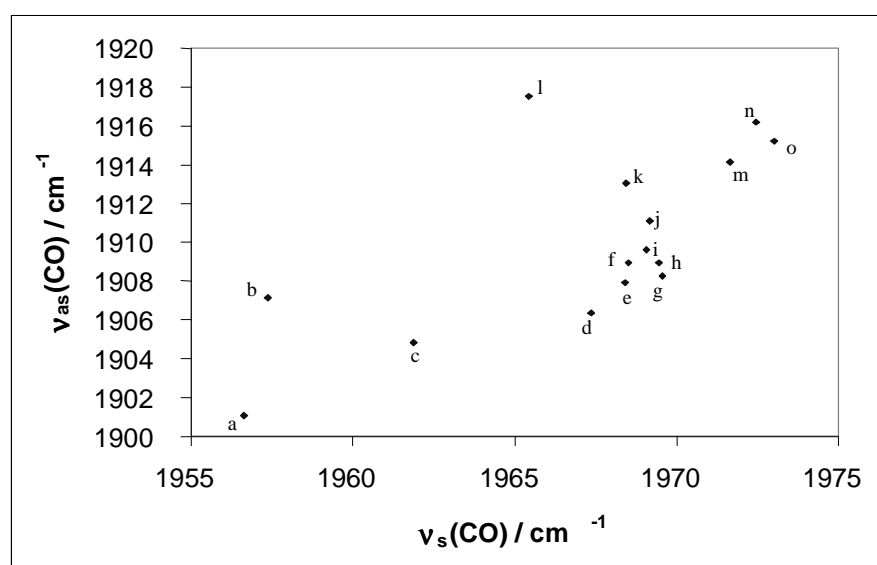


Fig. 11. Bellamy plot of $\nu_s(\text{CO})$ against $\nu_{as}(\text{CO})$ for complex **24** immobilised in silica nanoparticles and measured using the ATR optrode sensor; a = dioxane, b = dimethylformamide, c = dimethylsulphoxide, d = acetone, e = acetonitrile, f = dry, g = chloroform, h = dichloromethane, i = water, j = ethyl acetate, k = tetrahydrofuran, l = diethylether, m = methanol, n = dodecane, o = hexane.

At the present stage, the two comparisons presented here illustrate the value of calculations of normalised differential response ratios to quantify and compare the contributions of environmental effects on the relative positions of the $\nu(\text{CO})$ vibrational stretching modes of organometallic complexes.

4. Conclusions

The work described here is the next stage in our ongoing programme for the development of novel advanced materials for use in bioanalysis. We have progressed from simple combinations of molecular receptors and the carbonylmetal complexes that provide the IR read-out, to multi-carbonylmetal methods and supported molecular sensing devices. When multi-carbonylmetal methods are applied in bioanalysis, several independent sources of information are accessible in the same spectroscopic experiment, so direct effects arising from signal transduction of the host-guest chemistry of the receptor to the vibrational spectroscopy of the carbonylmetal component can be distinguished from general effects arising from random interactions with the diverse range of substances in the immediate environment of the probe group in a biological medium. This paper has provided further details of our work on the environment-induced effects. We have shown that relative wavenumber data can produce good correlations in Bellamy plots, and so allow the performance of different complexes to be compared, and that there are two important factors that bear on the degree of environment-sensitivity that can be expected. The range of extremes of response, and the variations of pairs of responses, are both important factors. The variability of rank orders of environment effects for different complexes can be studied by the calculation of normalised differential response ratios. We have demonstrated that in some cases very large discrepancies can be encountered in the relative positions of vibrational modes on the diagonals of the Bellamy plots for immobilised tricarbonyliron and dicarbonyl(triphenylphosphine)iron complexes. This is an essential first stage in the application of the FTIR optrode methodology to the analysis of biological systems. By a better understanding of the environment-induced changes, the interpretation of results from systems where solvent/media effects and receptor-originating effects are both operating (see Fig. 1) has been placed on a firmer footing, and we have a fuller understanding of how to design future functional materials for bioanalysis based on these principles.

We have also shown that ^{29}Si MAS NMR spectroscopy offers a powerful tool for the direct study of carbonylmetal complexes immobilised covalently on silica, and defined the position of the resonance of the additional silicon originating from the method of attachment of the metal complex. This characteristic resonance appears at about -20 ppm, approximately 80 ppm downfield from the Q^3/Q^4 silica resonances. DRIFT and transmission IR spectroscopy are also important for the characterisation of the covalently immobilised metal complexes, and relative peak heights from DRIFTS correlates with estimates of the quantities of the attached metal complexes determined by measurement of iron concentrations by AA spectroscopy. Integration of the -20 ppm ^{29}Si MAS NMR signal overestimates the surface-bound organometallic at high loadings.

Acknowledgement

This work was supported by EPSRC grant (GR/L75719). We thank BBRSC for support to CEA and the Royal Society for support to OE, the EPSRC National Mass Spectrometry Service Centre, University of Wales, Swansea, UK for high resolution mass spectrometric measurements, and J. Varga and J. Lejtovicz (Chemical Research Center of the Hungarian Academy of Sciences) for use of unpublished curve analysis software. Microanalysis was performed by Mr A.W.R. Saunders at the University of East Anglia.

References

- [1] J. H. Schneider, *Angew. Chem. Int. Ed. Engl.*, **32**, 848-850 (1993); W. Simon, *Chimia* **44**, 395 (1990); R. Murray, R. Dessy, W. Heineman, F. Janta, W.R. Seitz (Eds), *Chemical Sensors and Microinstrumentation*, ACS Symposium Series, **403** (1988); O.S. Wolfbeis, *J. Anal. Chem.* **337**, 522-527 (1990).
- [2] J. Janta, M. Josowicz, D. M. DeVaney, *Anal. Chem.* **56**, 179R-208R (1998); P. M. Saito, K. Kikuchi, *Opt. Rev.*, **5**, 527 (1997); M.N. Tulb, R. Narayanaswamy, *Analyst*, **120**, 1617 (1995); O.S. Wolfbeis, *Anal. Chem.*, **72**, 81R (2000); R. Narayanaswamy, *Analyst*, **118**, 317 (1993); T. Hao, X. Xing, C.C. Lui, *Sens. Actuators*, **10B**, 155 (1994).
- [3] M. J. P. Leiner, *Anal. Chim. Acta* **225**, 209, 1990.
- [4] O. Kazunori, R. Naganawa, H. Radecka, M. Kataoka, E. Kimura, T. Koike, K. Tohda, H. Furuta, *Supramol. Chem.*, **4**, 101 (1994); R.P. Buck, V. Cosofret, *Pure Appl. Chem.*, **65**, 1849 (1993); M. E. Collison, M. E. Meyerhoff, *Anal. Chem.*, **62**, 425 (1990); R. P. Buck, V. Cosofret, *Pure Appl. Chem.* 1993, **65**, 1849; O. Kazunori, R. Naganawa, H. Radecka, M. Kataoka, E. Kimura, T. Koike, K. Tohda, M. Tange, H. Furuta, *Supramol. Chem.* 1994, **4**, 101.
- [5] C. E. Anson, T. J. Baldwin, C. S. Creaser, G. R. Stephenson, *Organometallics* **15**, 1451 (1996).
- [6] M. Salmain, A. Vèssieres, G. Jaouen, I. S. Butler, *Anal. Chem.* **632**, 323-2329 (1991).
- [7] M. Salmain, A. Vèssieres, A. Varenne, P. Brossier, G. Jaouen, *J. Organomet. Chem.* **589**, 92 (1999).
- [8] C. S. Creaser, M. A. Fey, G. R. Stephenson, *Spectrochim. Acta* **50A**, 1295-1299 (1994).
- [9] C. E. Anson, C. S. Creaser, G. R. Stephenson, *J. Chem. Soc., Chem. Comm.* 2175-2176 (1994); C. E. Anson, C. S. Creaser, G. R. Stephenson, *Organometallics*, in preparation.
- [10] Diquat binding: C. E. Anson, C. S. Creaser, G. R. Stephenson, unpublished results [for the crown system on which this method was based, see: H. M. Colquhoun, E. P. Goodings, J.M. Maud, J. F. Stoddart, J. B. Wolstenholm, D. J. Williams, *J. Chem. Soc., Perkin Trans. 2*, 607 (1985)]; barbiturate binding: C. E. Anson, C. S. Creaser, G. R. Stephenson, unpublished results [for the host architecture on which this method was based, see: S.-K. Chang, D. Van Engen, E. Fan, A. D. Hamilton, *J. Am. Chem. Soc.*, **113**, 7640 (1991)].
- [11] C. E. Anson, C. S. Creaser, G. R. Stephenson, *Spectrochim. Acta* **52A**, 1183-1191 (1996).
- [12] C. S. Creaser, W. E. Hutchinson, G. R. Stephenson, *Appl. Spectrosc.* **54**, 1624-1628 (2000).
- [13] C. S. Creaser, W. E. Hutchinson, G. R. Stephenson, *Analyst* **126**, 647-651 (2001).
- [14] C. S. Creaser, W. E. Hutchinson, G. R. Stephenson, *Sens. Actuators* **82B**, 150-157 (2002).
- [15] L. J. Bellamy, R. L. Williams, *J. Chem. Soc.* 863 (1957); L. J. Bellamy, H. E. Hallam, R. L. Williams, *Trans. Faraday Soc.*, **54**, 1120 (1958); L. J. Bellamy, R. L. Williams, *Trans. Faraday Soc.*, **55**, 14 (1959).
- [16] D. A. Brown, H. Sloan, *J. Chem. Soc.* 3849 (1962).
- [17] A. V. Malkov, L. Mojovic, G. R. Stephenson, A. T. Turner, C. S. Creaser, *J. Organometal. Chem.*, **589**, 103-110 (1999).
- [18] A. J. Birch, D. H. Williamson, *J. Chem. Soc., Perkin Trans. 1*, 1892 (1973); B. M. R. Bandara, A. J. Birch, L. F. Kelly, *J. Org. Chem.* **49**, 2496-2498 (1984).
- [19] D. A. Owen, MSc Thesis, (1988) University of East Anglia, Norwich, UK [by a reported method: D. A. Owen, G. R. Stephenson, H. Finch, S. Swanson, *Tetrahedron Lett*, **30**, 2607 (1989)].
- [20] A. J. Birch, P. Dahler, A. S. Narula, G. R. Stephenson, *Tetrahedron Lett.* 3817-3820 (1980).
- [21] R. D. Nelson, D. R. Lide Jr, A. A. Maryott, *National Standards Reference Data Series*, National Bureau of Standards, **10** (1967).
- [22] *CRC Handbook of Chemistry and Physics*, CRC Press, Boston, USA, **72** nd Ed. (1991).
- [23] M. J. S. Dewar, J. P. Stewart, *Chem. Phys. Lett.* **111**, 416 (1984).
- [24] L. R. Snyder, *J. Chromatog. Sci.* **16**, 223 (1984).
- [25] C. E. Anson, C. S. Creaser, O. Eged, G. R. Stephenson, *Spectrochim. Acta* **53A**, 1867 (1997).

- [26] C. E. Anson, C. S. Creaser, J. A. Downie, O. Egyed, A. V. Malkov, L. Mojovic, G. R. Stephenson, A.T. Turner, K.E. Wilson, *Bioorg. Med. Chem. Lett.* **8**, 3549-3554 (1998).
- [27] C. E. Anson, C. S. Creaser, A. V. Malkov, L. Mojovic, G. R. Stephenson, *J. Organometal. Chem.* **668**, 101-122 (2003).
- [28] B. Buszowski, J. Schmid, K. Albert, E. Bayer, *J. Chromatog.* **552**, 415 (1991); B. Buszowski, M. Jaroniec, R. K. Gilpin, *J. Chromatog.* **673A**, 11 (1994); M. J. Cook, R. Hersans, J. McMurdo, D.A. Russell, *J. Mater. Chem.*, **6**, 415 (1996); T.G. Waddell, D.E. Leyden, M.T. DeBello, *J. Am. Chem. Soc.*, **103**, 5303-5307 (1981).
- [29] G. Engelhardt, D. Michel, *High-Resolution Solid State NMR of Silicates and Zeolites*, Wiley (1987) Chichester, UK.